J. Membrane Biol. 72, 117–130 (1983)

The Journal of
Membrane Biology

Interaction between Calcium Ions and Surface Charge as it Relates to Calcium Currents

D.L. Wilson, K. Morimoto, Y. Tsuda, and A.M. Brown
Department of Physiology and Biophysics, University of Texas Medical Branch, Galveston, Texas 77550

Summary. Calcium ions affect the gating of Ca currents. Surface charge is involved but to what extent is unknown. We have examined this, using isolated nerve cell bodies of *Helix aspersa* and the combined microelectrode-suction pipette method for voltage-clamp and internal perfusion. We found that Ba and Sr currents produced by substitution of these ions for extracellular Ca ions are activated at less positive potentials than Ca currents. Mg ions do not permeate the Ca channel and changes in $[Mg]_o$ produce shifts in the activation-potential curves that are comparable to the effects of changes in $[Ba]_o$ or $[Sr]_o$. Inactivation of Ba currents also occurs at less positive potentials. Perfusion intracellularly with EGTA reduced inactivation of Ca currents as a function of potential, but did not shift the inactivation-potential curve. Hence, Ca current-dependent inactivation which is blocked by intracellular EGTA probably does not involve a similar change of intracellular surface potential. The voltage shifts of activation and inactivation produced by extracellular divalent cations used singly or in mixtures can be described by the Gouy-Chapman theory for the diffuse double layer with binding (Gilbert & Ehrenstein, 1969; McLaughlin, Szabo & Eisenman, 1971). From the surface potential values and the Boltzman distribution, we have computed surface concentrations that predict the following experimental observations: 1) saturation of current-concentration relationships when surface potential is changing maximally; 2) the increase in peak current when Ca ions are replaced by Sr or Ba ions; and 3) the greater inhibitory effect of Mg on I_{Ba} than I_{Ca}. Theory indicates that surface charge cannot be screened completely even at 1 M $[Mg]_o$ and thus that Ca channel properties must be evaluated in the light of surface charge effects. For example, after correction for surface charge effects the relative permeabilities of Ca, Ba and Sr ions are equivalent. In the presence of Co ions, however, Ca ions are more permeable than Ba ions suggesting a channnel binding site may be involved.

Key words surface charge · surface concentration · calcium channels

Introduction

It is well-known that calcium ions alter the gating of Na channels (Frankenhauser & Hodgkin, 1957; Begenisich, 1975; Hille, Woodhull & Shapiro, 1975) and K channels (Gilbert & Ehrenstein, 1969; Mozhaeyeva & Naumov, 1970; Begenisich, 1975). The effects have been attributed to changes in surface potential near the Na and K channels and quantitative interpretations have been made based upon the Gouy-Chapman theory (GCt) of the diffuse double layer with binding (*see* McLaughlin, 1977, for a review). The situation is obviously more complicated for Ca channels since changes in extracellular Ca contentration, $[Ca]_o$, change the electrochemical potential of the current-carrying ions as well as the surface potential. Ohmori and Yoshii (1977) examined sodium and calcium channels in tunicate egg membranes when $[Ca]_o$ was changed and found similar shifts in the peak current-voltage relations ($I-V$'s) for both channels which were interpreted as voltage shifts in the gating parameters for the two channels. Kostyuk, Doroshenko and Ponomazev (1980) have recently reported comparable results for Ca currents in snail neurons.

In addition to an effect on gating, the presence of a negative surface charge should also affect the magnitude of the surface concentration of cations and thus the currents observed, particularly in the case of divalent cations. As pointed out by McLaughlin et al. (1971), at bulk concentrations of divalent cations where the surface potential is changing maximally, the surface concentration would tend to be independent of bulk concentration. An effect of this sort has been observed experimentally in gramicidin channels by Apell, Bamberg and Lauger (1979) and could provide an explanation for the saturation effects observed in the current-concentration relationships of the Ca channel (Kostyuk, Krishtal & Doroshenko, 1974; Hagiwara, 1975; Akaike, Lee & Brown, 1978). The divalent cations may also bind to the surface with different affinities, so that the relative concentrating effects at the surface would be affected by the divalent species present. Hence, for Ca channels

it is expected that surface charge effects should be important in determining the selectivity and saturation characteristics of the Ca channels as well as their gating characteristics. Some evidence for this was presented by Ohmori and Yoshii (1977) and Okamoto, Takahashi and Yamashita (1977) who found that the permeability sequences for the Ca channel of tunicate eggs and mammalian oocytes, respectively, were altered after correction of the surface concentrations.

Except for these studies, however, the action of Ca and other divalent cations upon Ca channel gating and Ca currents have been treated separately. The effects on gating have been attributed to changes in external surface potential (Kostyuk et al., 1974), and the effects on current have been ascribed to a channel binding site for which absorption is described by a Langmuir isotherm (Hagiwara, 1975; Akaike et al., 1978; Kostyuk, 1980). The present experiments examine both effects and illustrate how extracellular Ca ions regulate Ca influx. It was found that activation and inactivation gating were shifted by divalent cations and that Ca influx may remain relatively constant despite large changes in $[Ca]_o$. These results were explained by GCt with binding and a Ca channel binding site was not required to explain the saturating current-concentration relationships. Rather it appears that at and above the physiological range of $[Ca]_o$, the surface concentration of Ca ions is largely independent of the bulk concentration. Intracellular Ca ions also regulate Ca channel gating. A binding site with a high affinity for Ca_i seems to be present (Kostyuk, 1980) and accounts for Ca-current-dependent inactivation (Eckert & Tillotson, 1978; Tillotson, 1979; Brown, Morimoto, Tsuda & Wilson, 1981). However, this effect cannot be explained by surface charge effects on the inner surface of the membrane. In these different ways Ca ions regulate their own permeation via Ca channels. Preliminary results of this study have been reported previously (Brown, Tsuda, Morimoto & Wilson, 1982).

Materials and Methods

Experimental

The experiments were done on isolated nerve cell bodies of *Helix aspersa* using the combined microelectrode-suction pipette method of internal perfusion and voltage clamp described in Brown et al. (1981). The microelectrode measured the membrane potential and the suction pipette was used for passing current and internal perfusion. Details of the suction pipette construction are included in Lee, Akaike and Brown (1980). Ca tail currents were measured to obtain activation-potential curves. These tail currents are large and fast (Byerly & Hagiwara, 1982; Tsuda, Wilson & Brown, 1982) and thus require a careful analysis of the voltage-clamp system. Our methods for such studies will be described fully in a forthcoming paper (Brown, Tsuda & Wilson, *manuscript in preparation*). For such experiments, where clamp speed was important, the microelectrode was coated with silver paint, insulated and connected to a negative capacitance compensation network. With this system voltage steps were attained within 20 μsec and the large, fast initial component of the capacitative transient was 90% complete in about 60 μsec. Series resistance R_s measured with impedance methods was estimated to be less than 5 kΩ and measurements of membrane potential with a second microelectrode "outside" the clamp system indicated that spatial control to within 0.3 mV was attained within 100 μsec.

Ca currents I_{Ca} were isolated as described by Brown et al. (1981). K currents were suppressed by Cs substitution for K ions, TEA intra- and extracellularly and 4-AP extracellularly. Na currents were suppressed by Tris substitution. Linear components of leakage and capacitive currents were subtracted by adding voltage steps of equal amplitude and opposite sign. At potentials above +40 to +50 mV, a small nonspecific voltage and time-dependent current I_{NS} was present. This current was measured by substituting 10 Co for the permeable species (Brown et al., 1981), and in some cases it was subtracted from the currents of interest. This correction was found to have little or no effect at the voltage for the peak inward current, the voltage range primarily used in this study, and thus it was not always done. In cases where such a correction was not made we have truncated the plots of the $I-V$ curves at potentials above which corrections would be significant. The basic extracellular solution in mM was Tris-Cl 35, TEA-Cl 50, CsCl 5, 4-AP 5, glucose 5.5, $CaCl_2$ 10, and $MgCl_2$ 15 and the intracellular solution was CsAsp 135 and TEA-OH 20. pH of the extracellular and intracellular solutions was adjusted to be 7.2 and 7.5, respectively. Different extracellular concentrations of divalent cations are indicated in the text and figure legends. Each change was followed by restoration of the control solution and the current-voltage relationships were redetermined. Experiments were done at a room temperature of 22 to 23 °C.

Steady-state activation was estimated from tail current amplitudes. These were measured at the holding potential V_H of −50 mV (Figs. 3 and 4) after a 5-msec depolarizing pulse. V_H corresponds to the resting potential of about −50 mV in the solutions used to isolate I_{Ca}, and holding currents of less than 10^{-9} A were required for this V_H. Steady-state inactivation, the h_∞ parameter in Hodgkin-Huxley notation (1952), was determined with the usual two-pulse paradigm (Fig. 7) and required conditioning pulses of one to several seconds in duration.

Theoretical

The data were analyzed using a modification of the Gouy-Chapman equation that includes specific binding. The modification was developed by Stern (1924) and was first applied to excitable membranes by Gilbert and Ehrenstein (1969). The Gouy-Chapman equation is derived for the case of a half-space of ionic solution bounded by a uniform, planar surface charge, and it is simply the solution of the Poisson equation with the charge distribution given by the Boltzmann relation. In a form derived by Grahame (1947) for solutions of mixed electrolytes, the Gouy-Chapman equation relates the surface potential Ψ (the electrical potential between the solution bulk phase and the surface) with the bulk concentration of each ionic species C_j and the surface charge density σ. The equation is

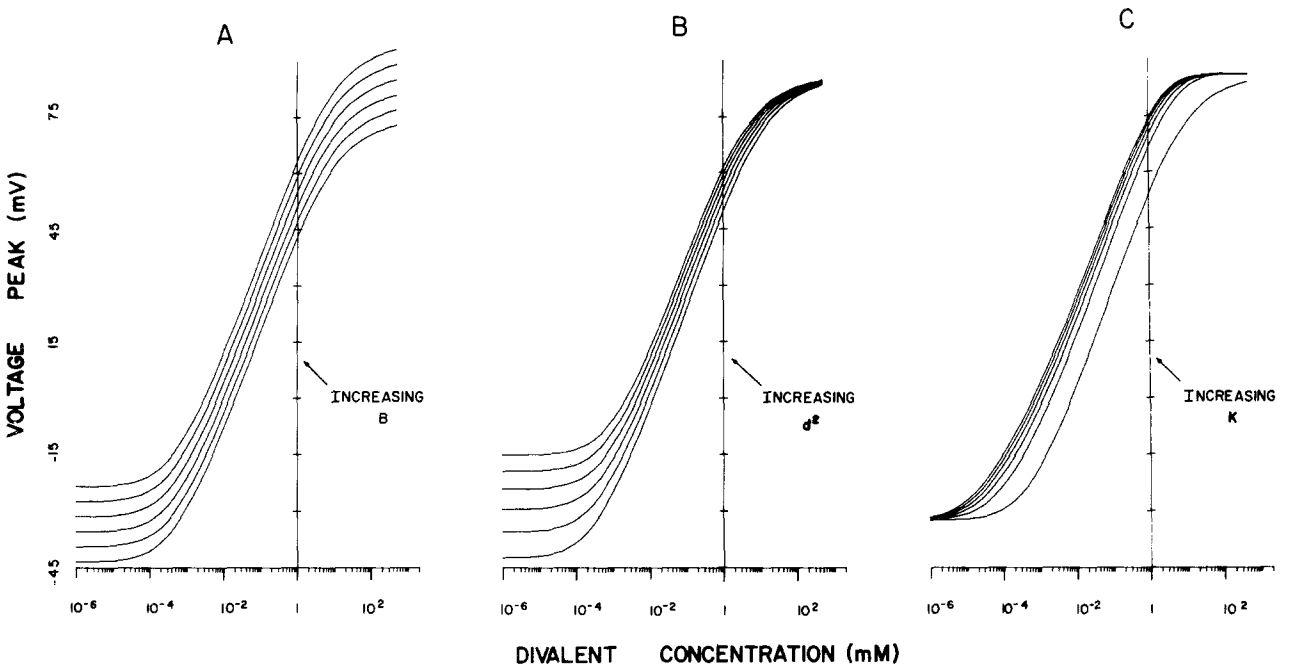

Fig. 1. Plots that show how the parameters in Eq. (5) of the text affect the peak voltage versus concentration relationship. Nominal values are $B=86$ mV, $d^2=80\ e/\text{Å}^2$, and $K=0$ molar^{-1}. *A.* "B" is varied from 75 to 95 mV in steps of 4. *B.* "d^2" is varied from 65 to 115 $e/\text{Å}^2$ in steps of 10. *C.* "K" is varied from 0.0 to 1.0 molar^{-1} in steps of 0.2

$$\sigma=\frac{1}{G}\left\{\sum_{j=1}^{n} C_j[\exp(-z_j H\Psi)-1]\right\}^{\frac{1}{2}} \tag{1}$$

where G is a constant comprised of several physical constants and has a value of 270 (Å^2/charge) (mole/liter)$^{1/2}$, z is valence, and H has a value of 1/25 mV^{-1} at room temperature. Boltzmann's relation is

$$C_i(x)=C_i(\infty)e^{-U(x)H} \tag{2}$$

where $U(x)$ is the potential seen by the ion as a function of distance from the surface x. In the derivation of Gouy-Chapman equation, it is assumed that $U(x)$ is just the mean electrostatic potential. Thus, at the surface we have

$$C_i(o)=C_i(\infty)e^{-Z_i\Psi(o)H}. \tag{3}$$

We assume that the divalent cations bind with divalent anionic sites on the membrane suface as described by Gilbert and Ehrenstein (1969), and we obtain

$$\frac{\sigma}{\sigma_t}=\frac{1}{1+\sum_{i=1}^{m} K_i C_i(x=0)} \tag{4}$$

where σ_t is the total negative surface charge, σ is the amount left after binding, K_i is the association constant and we have allowed for more than one binding species. We now combine Eqs. (1), (3) and (4) to obtain our working equation

$$d^2\sum_{i=1}^{m}[K_i C_i e^{-Z_i H(V_p-B)}+1]=\frac{G}{\left\{\sum_{j=1}^{n} C_j[e^{-Z_j H(V_p-B)}-1]\right\}^{\frac{1}{2}}} \tag{5}$$

where we have expressed the surface charge in terms of d^2, which is the effective distance squared between charges and we have set Ψ equal to V_p-B, where V_p is the voltage of the maximum inward current on the peak $I-V$ curve. The internal surface potential Ψ_i is assumed to stay constant during external solution changes and is for the moment included in B which is the value of the membrane potential corrected for the surface potential that acts on the Ca channel gating mechanism at V_p. The use of V_p is justified in a later section.

Equation (5) may not be solved explicitly for V_p as a function of divalent concentration. We therefore used a modified Newton-Raphson root searching technique for numerical evaluation of V_p as a function of bulk concentrations. Equation (3) may then be used to evaluate the free surface concentration of the ionic species available for permeation of the Ca channel.

We used one variation of this basic model for fitting some of the data to account for a reduction in concentration at the mouth of the Ca channel. Apell et al. (1979) calculated the potential at the center of a charge-free disk (the channel mouth) in a plane covered with a smeared surface charge using the linearized Poisson-Boltzman relation which assumes that the surface potential Ψ is much less than RT/F. Their result is

$$\Psi_c=\Psi_{\text{surf}}e^{-r_c/L_D} \tag{6}$$

where Ψ_c is the potential at the center of the disk, Ψ_{surf} is the surface potential far away from the disk, r_c is the disk radius and L_D is the Debye length. This seems a reasonable model for finding the potential at the center of the channel mouth and we used Ψ_c in the Boltzman relation to find the concentration there. We thus evaluated Ψ_{surf} from Eq. (5), and Ψ_c from Eq. (6), and we then applied the Boltzmann relation to each permeable species to find the concentration of permeable ions at the channel mouth.

Next we compared the surface concentration predictions with the peak currents obtained for divalent ions that permeate the Ca channel. Implicit in this comparison are the assumptions that the currents obey the Independence Principle and that the outward current is negligible. We note that Cs ions do not carry outward current through the Ca channel (Brown et al., 1981) and Ca outward current is expected to be negligible at the voltages where peak currents occur given the Ca$_i$ activity

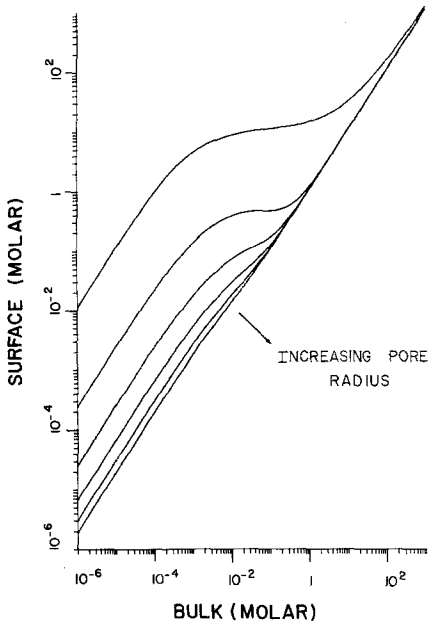

Fig. 2. Plots of the prediction of the concentration at the center of the pore as a function of the bulk concentration with the pore radius varied from 0 to 24.5 Å in steps of 4.9 Å. The monovalent concentration was 100 mM and the other parameters are the same as in Fig. 1

of 10^{-8} M. Support for the latter assumption comes from the observation that a calculation of the current-voltage relationship from the constant field equation indicates that the outward Ca flux will be negligible over the voltage range studied, and outward Ca current has not been measured (Akaike et al., 1978; Kostyuk, 1980; Hagiwara & Byerly, 1981).

We implemented the models in a computer routine which allowed plotting on a CRT screen of the theoretical curves superimposed with the data points. Parameters were estimated by varying them until a good visual fit was achieved. In Fig. 1 a sample output is shown which allows us to see the effect of varying parameters d^2, B and K. We have plotted these values over an extended range to aid in the physical interpretation. We see that there are two asymptotic values of V_p as expected. At very low concentrations screening does not occur and at high concentrations the surface potential has been reduced to zero. In Fig. 1 left, we note that the high concentration asymptote is given by the value of B, and B can therefore be interpreted as the "true" potential, that is, the potential across the membrane after the surface potential has been eliminated. In Fig. 1 middle, we see that d^2 affects the total distance between the asymptotes in the manner expected; that is, increasing d^2 decreases the effective surface charge and therefore reduced the maximum change in V_p. The value of d^2 also determines where the initial upswing of the curve occurs. In Fig. 1 right, an increasing value of K simply makes the curve begin the upswing at a lower concentration.

In Fig. 2, we have plotted the predicted surface concentration vs. the bulk concentration as a function of the pore radius. At low bulk concentrations, the surface concentration is much higher than the bulk, but at higher bulk concentrations the surface concentration asymptotically approaches the bulk concentration. Increasing the pore radius decreases the concentrating effect at the center of the pore as expected. Note that the most horizontal portions of the curves occur in the physiological range of concentrations and coincide with the portions of the voltage-concentration curves that have the steepest ascent, as predicted by McLaughlin et al. (1971).

Results

There are two sets of results that require interpretation: voltage shifts of Ca channel gating parameters produced by divalent cations and current flow through channels as a function of divalent cation concentration. These will be presented in order and compared with predictions of surface potential and surface concentration made by the Gouy-Chapman equation with binding.

Voltage Shifts in Ca Channel Gating Parameters

Shifts in Activation Gating. Increases in $[Ca]_o$ increase the peak Ca currents and shift the I–V relationship to more positive potentials (Figs. 3*B* and 6*A*). Increases in $[Ba]_o$ and $[Sr]_o$ have similar effects but compared to the $I-V$ curves for I_{Ca} the Ba and Sr curves are displaced to less positive potentials (Figs. 4*A*, 6*B* and *C*). The shift of the Sr $I-V$'s are similar to those of Ba under the solution conditions of our experiments, and results for Sr currents are considered together with those for Ba currents,. Subsequently, it will be shown that Mg ions can cause shifts in Ba current (Fig. 5) and smaller shifts in Ca current (Fig. 8*B*) and that adding Ca ions can cause a shift of the $I-V$ obtained in a mixture of Ca and Ba ions (Fig. 10*B*). These effects are completely reversible. For example, the $I-V$ curves shown in Fig. 4*A* were obtained at 10 mM divalent cation concentration, the control value. $I-V$ curves similar to these can be reproduced for 6 to 8 hr in healthy cells, the latter being cells with resting potentials of approximately -50 mV, action potential amplitudes >80 mV and input resistances of 5 to 10 MΩ. The data resulting from a solution change were used only if the $I-V$ curves following restoration of the control solution were similar to the control curves.

The most direct tests of shifts in activation gating were achieved by tail current measurements. Ca current was activated by a 5-msec depolarizing potential step; this duration is sufficient to reach the peak of the inward current and indicates that a steady state of activation has been attained. The amplitude of the tail current immediately upon return to the V_H of -50 mV is much greater than the amplitude of the peak current, and the tail amplitude was used to estimate the extent of activation during the depolarizing step. In our experiments, the tail currents were corrected to remove the linear capacitative and leakage components by summation of hyperpolarizing and depolarizing pulses. The contribution of asymmetric currents (Kostyuk, Krishtal & Pidoplichko, 1981) to the tail currents has been evaluated and was small

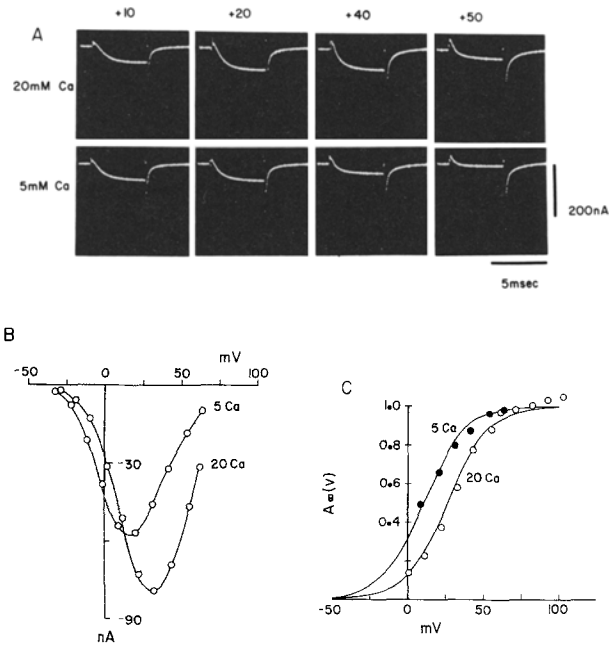

Fig. 3. Effect of Ca_o on activation. The current records and the resulting peak $I-V$'s obtained in 5 and 20 mM $[Ca]_o$ in the presence of 15 mM $[Mg]_o$ are shown in *A* and *B*, respectively. Peak $I-V$'s are not corrected for I_{NS} leakage currents which are obtained after Ca replacement by Co as described by Brown et al. (1981). V_H was -50 mV and the step potentials are indicated. At these pulse durations peak current was reached. The tail current decays in two phases. Many points in the fast phase of decay have not reproduced. In *C* the normalized amplitude of the fast exponential obtained from the fits of the tail currents is plotted against potential to give an activation curve. In general the activation curves saturated at high potentials as shown here in the case of 5 mM Ca and in Fig. 4. This was verified both from the exponential fits and from overlaying original data traces. We feel that the slight continuing increase in the 20-mM Ca activation curve is probably due to inaccuracies in measuring the fast component of the tail currents rather than a physical property of the membrane. (The smooth curves in *C* were made with a K value of 13.5 mV^{-1} and V' values of 10 and 26 mV for 5 and 20 mM $[Ca]_o$, respectively.)

enough to be ignored (Tsuda et al., 1982). With short pulses of 5-msec duration, the tail current relaxes in two phases, both of which are abolished by replacement of Co for external Ca, and we have fit these tail currents with the sum of two exponentials. The amplitude associated with each exponential is a function of the pulse potential as described for other voltage-activated currents, and we thus make the usual assumption that the amplitude measures the amount of activation immediately preceding the step in potential back to V_H. A detailed description of the tail currents is forthcoming (Brown, Tsuda & Wilson, *manuscript in preparation*). We present here the data obtained from the fastest exponential because it is indisputably linked to Ca current activation (Byerly & Hagiwara, 1982; Wilson, Tsuda & Brown, 1982). More-

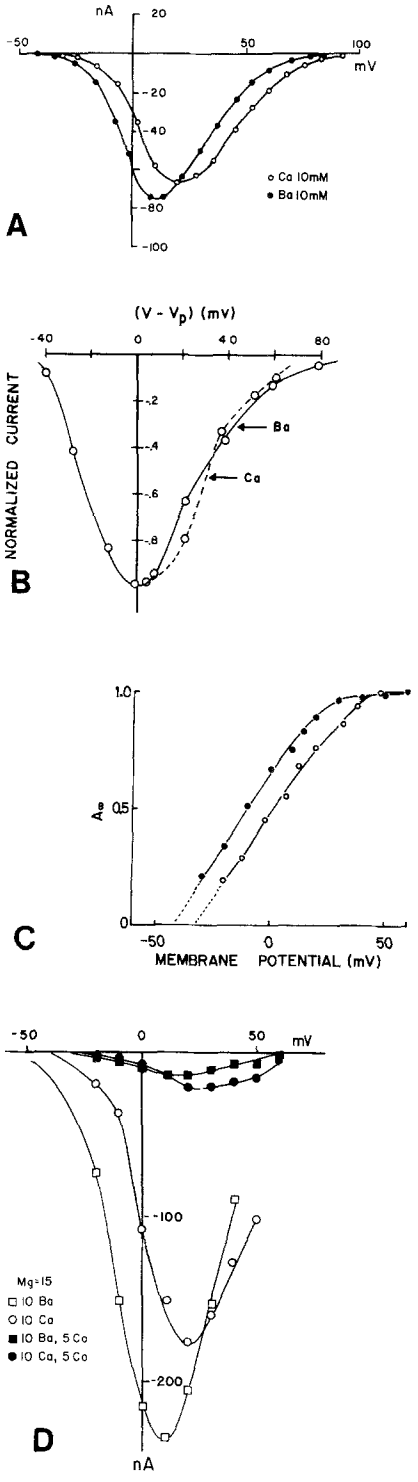

Fig. 4. A comparison of the voltage dependence of I_{Ba} and I_{Ca}. *A*. Leak corrected $I-V$ relationships for peak currents measured in Ba and Ca. *B*. Same $I-V$'s which have been normalized to 1.0 and shifted along the voltage axis to the origin. The curves overlay almost exactly indicating that threshold is shifted the same as V_p and suggesting that current-concentration relationships are not voltage dependent. *C*. Activation curves obtained by normalizing the tail current values. *D*. Comparison of effects of 5 mM Co on I_{Ba} and I_{Ca}. The relative reduction of I_{Ba} is much greater, and, in the presence of $[Co]_o$, I_{Ca} is larger than I_{Ba}

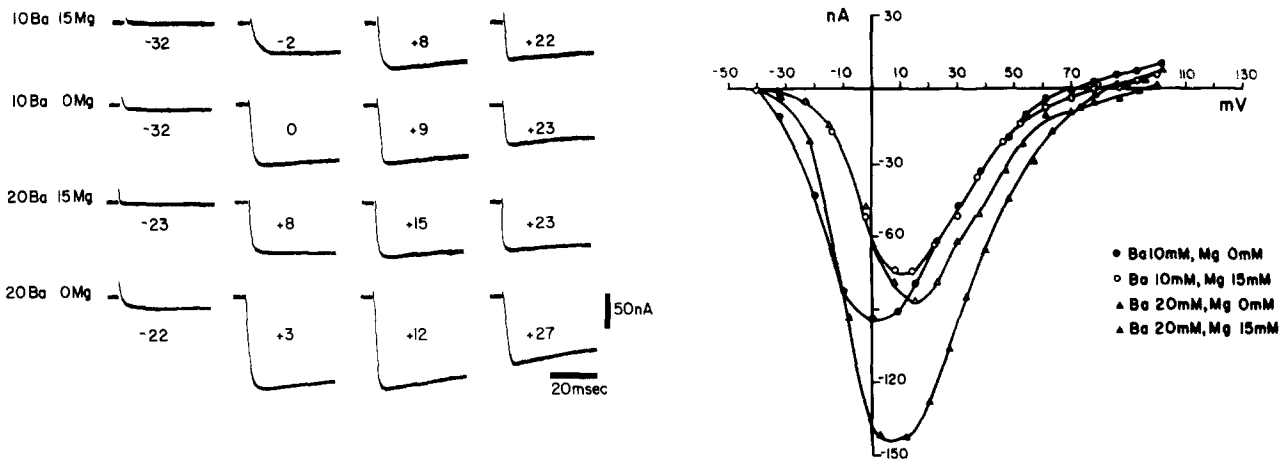

Fig. 5. Effect of $[Mg]_o$ on I_{Ba} at Ba concentrations of 10 and 20 mM. The shift and amplitude change of the peak currents are observable in both the peak $I-V$ curves and the raw data. $I-V$'s are not corrected for I_{NS} leakage current

over, its amplitude is 4 to 5 times larger than the amplitude of the slow component; thus it would tend to dominate if we used the sum of the two amplitudes. The amplitude of the normalized fast component is shown in Fig. 3*C* and it is called $A_\infty(v)$. These curves were fit using the following expression

$$A_\infty(v) = \{1 + \exp[K(V' - V_m)]\}^{-1} \quad (7)$$

and the parameters are indicated in the figure legend. Note that the $A_\infty(v)$ curve does not reach 1.0 until approximately +40 to +60 mV. The shift of the $A_\infty(v)$ curve is 16 mV as measured from the parameters indicated. The shift in the peak of the $I-V$ curve referred to as V_{peak} or V_p is 15 mV (Fig. 3*B*) and the shift in the half-maximal potential, $V_{1/2}$, for the descending limb of the $I-V$ curve is 14 mV. The above results thus indicate that the shape of the entire $I-V$ is affected by the activation function and explain why a shift in the peak of the $I-V$ curve reflects a shift in the activation function.

In Fig. 4 a similar analysis is done to compare Ca and Ba currents. In this case the data were not stored digitally so analysis was done by hand from semilogarithmic plots. The shift in the activation curves V_p and $V_{1/2}$ are once again similar. In Fig. 4*B* we have plotted the $I-V$'s after normalizing to the peak current and shifting the $I-V$ peaks along the voltage axis to 0 mV. The descending limbs of the resulting curves were indistinguishable and the ascending portions have approximately the same values. This was a fairly consistent result in experiments using relatively small changes (<15 mM) in divalent ions. With larger changes, the descending portion overlapped quite well, but the overlap for the ascending portions, although good, may not be exact. In these cases a possible explanation may be that the $I-V$'s were not corrected for the nonspecific current I_{NS}, which contaminates Ca currents at potentials above +30 mV (Brown et al., 1981). We have not studied the effects of these solutions on I_{NS}. Thus, the measured effect on the $I-V$'s of varying external divalents may be described simply by a parallel shift in the $I-V$ curve and a scaling of the current amplitude. It does not appear that changes in the Nernst potential of the current-carrying species produced significant effects on V_p and $V_{1/2}$.

It is also possible to examine voltage shifting using the nonpermeant divalent cation Mg. In Fig. 5 we see both from the raw data and the $I-V$ curves that when Mg is increased externally there is a voltage shift in both the peak of the $I-V$ and the voltage where the inward current first begins to appear. Note also that there is a reduction in the peak current when Mg is applied. In addition, note that when Ba is increased from 10 to 20 mM, the increase in current is much greater when Mg is absent than when it is present. Since Mg does not permeate the Ca channel (Akaike et al., 1978), this is clear evidence that the shift in the $I-V$ may occur when there is no change in the Nernst potential of the permeant ion. Later we will see that the shift in V_p caused by adding Mg to a Ba solution is equivalent to the shift in V_p caused by adding equimolar Ba. Similarly, in Fig. 4 we have shown that the Ca $I-V$ is shifted to the right of the Ba $I-V$ despite the fact that the external divalent concentrations are equivalent. These results are consistent with the idea that the shift is not resulting from a change in driving force but instead is due to a shift in voltage-dependent parameters, specifically the activation parameters.

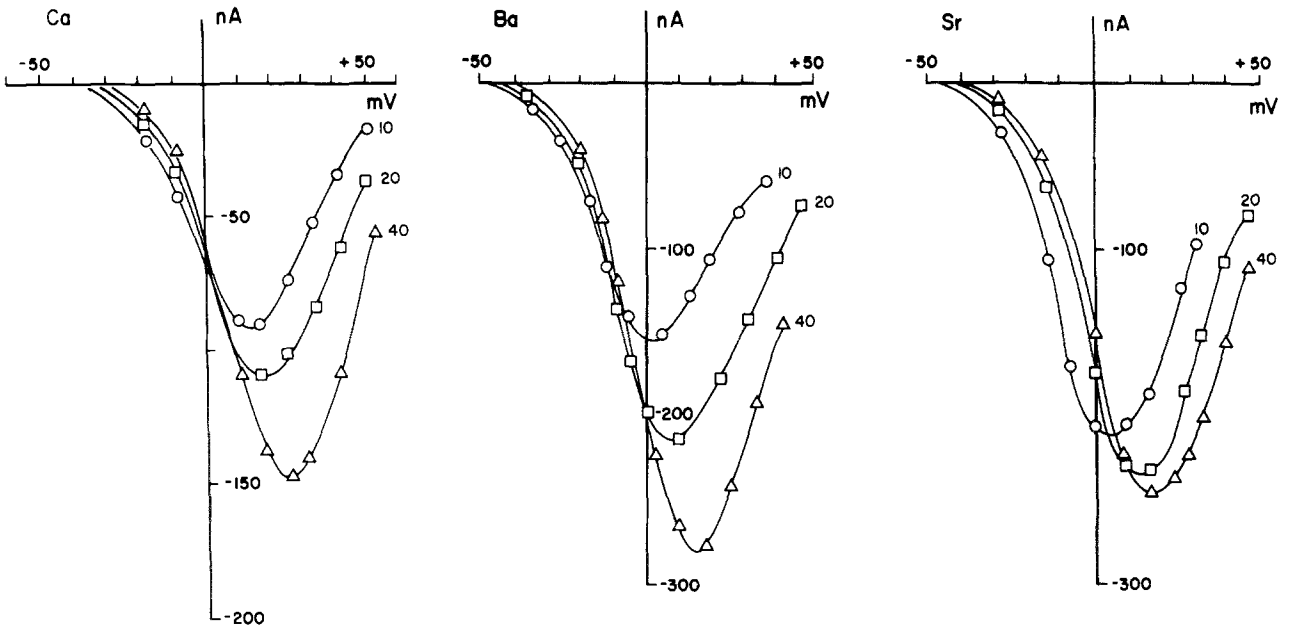

Fig. 6. Current-voltage relationships ($I-V$'s) without leakage correction plotted as a function of the external divalent concentration (in mM). Currents were normalized to the usual current (100 nA) obtained in a control solutions so that corrections could be made for slow decreases in the current that occurred over the course of these long experiments. Compared to Ba or Sr, Ca currents are smaller and shifted to the right. (Data from 3 cells.)

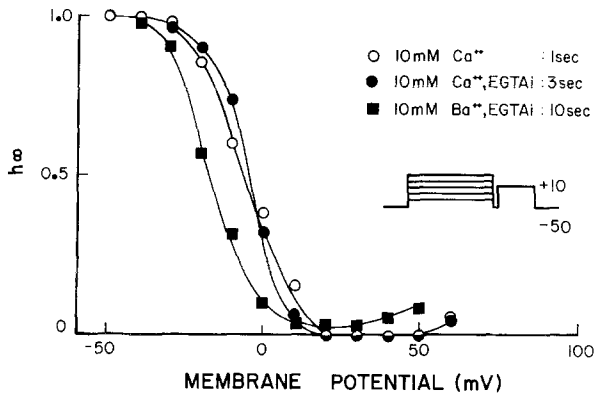

Fig. 7. A comparison between the inactivation of I_{Ba} and I_{Ca}. The pulsing scheme is shown in the inset and the peak current in the test pulse normalized by the control current in a test pulse is called h_∞. The prepulse durations required to attain steady-state inactivation are shown. Note that the h_∞ curve obtained with Ca present is shifted to the right of the curve obtained with Ba present. Addition of EGTA to the internal perfusion solution had no significant effect on $h_\infty(V)$ for I_{Ca}

Since the voltage shifts of V_p and $V_{1/2}$, measured from the $I-V$ curves, are identical and appear to be the same as the voltage shifts measured from the activation curve, we use V_p for our reference point for making the voltage shift measurements. The practical consequence of this was that more experimental data could be evaluated since we had accumulated a large number of $I-V$ curves for a variety of divalent cations and mixtures of divalent cations. Additionally, the measurements from the peak currents are themselves probably more reliable than the measurements from the tail currents. The $I-V$ curves for Ca, Ba and Sr currents produced at three different extracellular concentrations are shown in Fig. 6.

Shifts in activation gating were also produced by addition of submaximal doses of Ca channel-blocking divalent cations such as Co. However, the currents were too small to make accurate estimates of voltage shifting (Fig. 4*D*). What is obvious is that peak Ba currents are smaller than peak Ca currents after the addition of Co. This is a result that cannot be obtained with GCt with binding, thus indicating that Co may have an effect on the Ca channel in addition to its action on surface charge.

While activation of the Ca channel appears to be exclusively potential-dependent, inactivation is both Ca current-dependent and voltage-dependent (Brown et al., 1981). Ba current-dependent inactivation is minimal if it exists at all. Therefore, the shift in the inactivation gating parameter $h_\infty(V)$ between I_{Ca} and I_{Ba} might differ from the shift in activation. The results shown in Fig. 7 indicate that this is not the case. Since I_{Ca} and I_{Ba} inactivate at much different rates, we decided to obtain two curves with prepulses just long enough to make h_∞ reach zero between +20 to +50 mV. In the case of I_{Ca}, the potential at which $h_\infty(V)$ is 0.5,

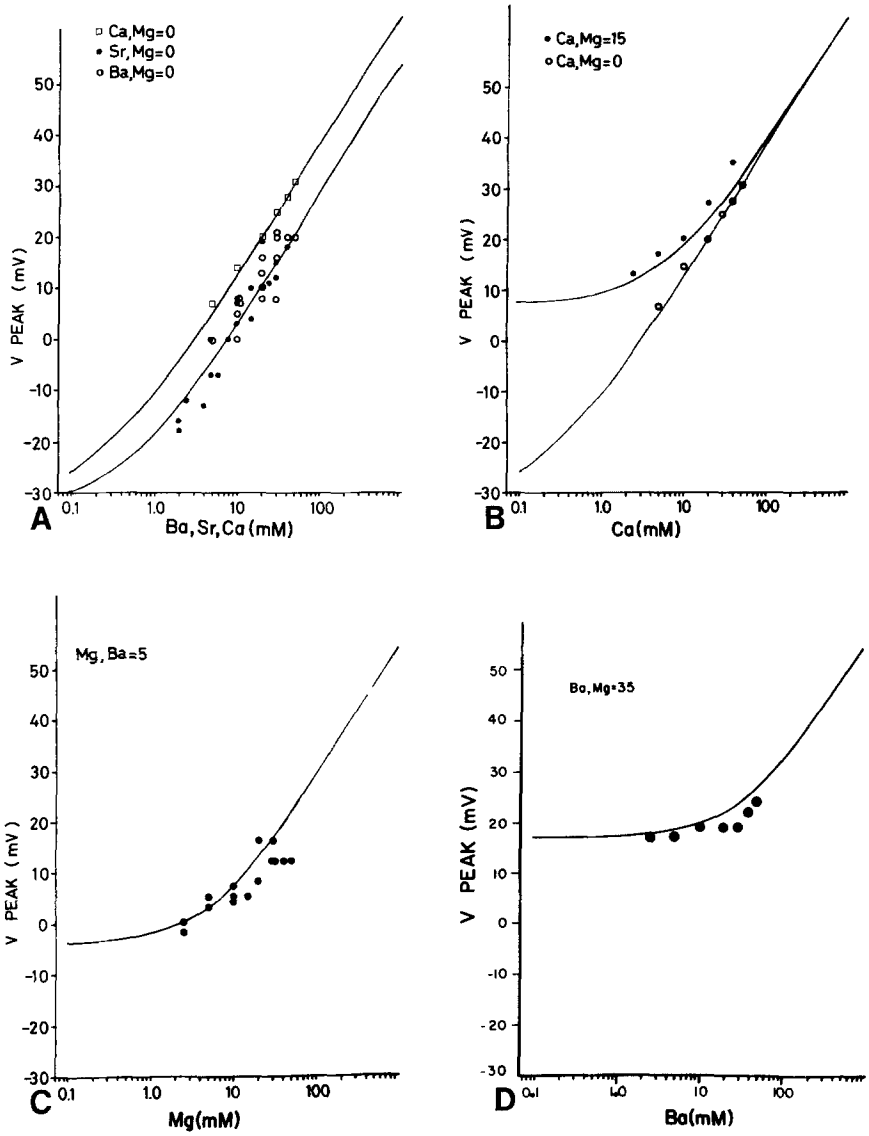

Fig. 8. Comparison of experimental results and theory for shifts in activation gating as measured from the peak of the $I-V$ curve. Parameters for the theoretical curves are $d^2 = 1/80\ e/\text{Å}^2$, $B = 86$ mV, and $K_{Ca} = 0.1$ molar^{-1}; species other than Ca are assumed not to bind. (Data are pooled measurements from 8 cells.) *A*. V_{peak} values for I_{Ca}, I_{Ba} and I_{Sr} in the absence of Mg. *B*. V_{peak} plotted as a function of Ca concentration in zero and 15 mM $[Mg]_o$. *C*. V_{peak} produced by varying $[Mg]_o$ at a constant $[Ba]_o$ of 5 mM. *D*. V_{peak} produced by varying $[Ba]_o$ at constant $[Mg]_o$ of 35 mM

$V_{1/2}$ for $h_\infty(V)$, is about 10 mV more positive than $V_{1/2}$ for I_{Ba}, and this result does not change significantly for prepulses longer than those indicated. For comparison, the shift in the activation curve for I_{Ba} and I_{Ca} at similar extracellular concentrations is 11 mV (Fig. 4), almost identical to the shift in $h_\infty(V)$. Adding EGTA to the intracellular perfusate reduces Ca current-dependent inactivation (Brown et al., 1981) and hence the prepulse duration was increased from 1 to 3 sec, to reach the required inactivation level. Note that no voltage shifting results from the addition of $EGTA_i$. Additionally, $EGTA_i$ did not significantly shift the peak $I-V$ curves. These results indicate negligible surface potential effects of Ca ions on the inside of the cell membrane.

Relationship between Shifts in Activation Potentials, Bulk Concentrations and Gouy-Chapman Theory

We first fitted the voltage shift data for Ba, Sr and Mg assuming no binding using Eq. (5). In this case we may vary d^2 and B only because we assume no surface binding by these ions. After several iterations, a reasonable fit was obtained and these parameters were now fixed. We then fit the data for Ca by simply varying the corresponding binding constant. The results are shown in Fig. 8. We were able to get excellent fits for the voltage shifts produced by Ca, Ba, Sr and Mg. The fits gave values for σ of $1e^-/80\ \text{Å}^2$, a maximum Ψ of -116 mV, a value for B of $+86.8$ mV and a

binding constant for Ca of 0.1 M^{-1}. The values for Ψ, σ and K_{Ca} are similar to those observed by Ohmori and Yoshii (1977) for tunicate egg Ca and Na channels, and they are also comparable to similar values for Na and K channels reported in the literature (Gilbert & Ehrenstein, 1969; Hille et al., 1975).

In addition to single ion experiments, we also had several experiments in which effects from more than one divalent ion were combined. In these instances, the theoretical curves were plotted using parameters already set in previous single ion experiments; there were no free parameters. For example, we studied the effects of varying $[Mg]_o$ at constant $[Ba]_o$ (Fig. 8*C*) and/or varying $[Ba]_o$ at constant $[Mg]_o$ (Fig. 8*D*). The data were fit quite well by theory. From these two Figures, we see that both the data and theory indicate that voltage shifting still occurs at 30 to 50 mM $[Mg]_o$, and the extrapolated theoretical curves indicate no signs of levelling off even at values of 1 M. Thus, it would be virtually impossible to screen all the surface charge even with high concentrations of Mg ion. In Fig. 8*B* we show the voltage shifting of the I_{Ca} peak with and without Mg present, and again the results were fitted by the theory. An alternative explanation is possible, however (*see* McLaughlin et al., 1981). The divalent cations could have combined not with a divalent anionic site but rather with a monovalent anionic site. Charge reversal would occur and the effects of Mg would continue to occur.

The shifts in the Ca channel current reflect the effects of changes in the surface potential rather than changes in the concentration gradient that occur as we vary the concentration of the external permeable divalent cation. As we have indicated the surface concentration of divalent cations is strongly dependent on the factors which affect surface potential – the amount of surface charge present, the amount of screening and the amount of binding. Also because of the greater electrostatic attraction, these effects are much greater on divalents than monovalents such as Na or K (Eq. 3). The effects of changes in surface potential on surface concentrations of free divalent ions are examined in the next section.

Current-Concentration Relationships

The saturation of Ca current at increasing $[Ca]_o$ has been reported by several authors (Kostyuk et al., 1974; Hagiwara, 1975; Akaike et al., 1978). We decided to test whether the changes in peak current may simply reflect the changes in the surface concentration of the permeable ions. Because the normalized and shifted $I-V$'s tend to overlap, it appears that the normalized $I-V$ relation is comprised of an activation function (as noted earlier, inactivation is negligible at the time of peak current) and a normalized instantaneous $I-V$ function that shift along the voltage axis by almost equivalent amounts. This may be expected to be the case, since a change in the surface potential would be expected to shift the instantaneous $I-V$ curve just as it would the activation curve. We can show how this might be expected to work for the case where we assume the $I-V$ relation to be given by the following equation

$$I=\frac{A_\infty(V-\Psi)\cdot(V-\Psi)\cdot P}{1-\exp[2(V-\Psi)F/RT]} \quad C(x=0). \tag{8}$$

This equation was formed from the product of the activation function, $A_\infty(E-\Psi)$, and the constant field equation where P is a constant and the other variables have been previously defined. In Eq. (8) we have assumed the outward flux to be zero and we have applied the usual adjustments for surface charge effects (Frankenhaeuser, 1960; Ohmori & Yoshi, 1977), that is, we have set the external concentration equal to the surface concentration and we have subtracted the voltage drop given by Ψ. The assumption of zero outward flux is substantiated by the result that at the potentials of interest the term in the constant field equation due to the outward going flux is negligible because of the low internal Ca concentration (10^{-8} M). From Eq. (8), we can see that $I_{Ca}/C(x=0)$ would be expected to be a constant function which is simply shifted along the voltage axis as a function of Ψ. Thus, we may proceed with the analysis assuming that the peak current reflects the surface concentration, and we will attempt to see if the surface concentration values predict quantitatively the saturation and selectivity characteristics of the Ca channel.

Peak currents as a function of $[Ba]_o$, $[Sr]_o$ and $[Ca]_o$ are shown in Fig. 9*A* and *B*, and the effects of Mg, a nonpermeating divalent cation, upon current-concentration curves are also illustrated. Concentration values on the abscissa are the bulk concentration values of the permeable species. In frames *C* and *D* of Fig. 9, we have plotted the theoretical surface concentration curves of the permeable species calculated with and without the charge-free disk modification (radius of 6.9 Å) and these are indicated "pore" and "no pore," respectively. We have plotted the curves such as to allow a comparison of the shape of the surface concen-

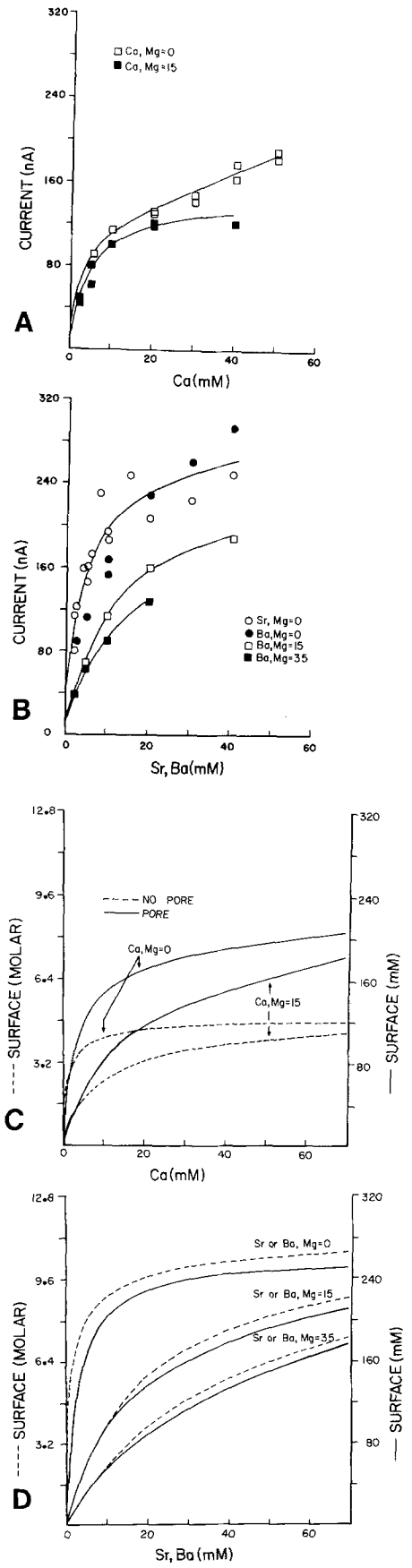

Fig. 9. Comparison of the experimental peak current-concentration relationship and the theoretical predictions for the surface concentrations. In *A* and *B* experimental data are plotted and the smooth curves have no theoretical significance. We saw no consistent differences between Ba and Sr and we show only one smooth curve through the middle of the points. In *C* and *D* we show predictions of the surface concentrations for the cases where the pore, or charge-free disk, is present and where it is absent, and the predictions are presented for the experimental conditions in *A* and *B*, respectively. The surface concentrations were plotted on scales such that one may compare the shape of the curves with the measured current-concentration curves in *A* and *B*. Parameters are the same as in Fig. 7 and the pore radius is 6.9 Å. (Data are pooled from 7 cells.)

tration curves with the current-concentration curves. The basic aspects of both sets of theoretical results agree with the data. That is, at the higher bulk concentrations, I_{Ba} and I_{Sr} are greater than I_{Ca} and the predicted surface concentrations are also greater. Also, Mg has a greater effect on I_{Ba} than I_{Ca} in both the current-concentration data and the theoretical surface concentration predictions. Unlike Co, Mg does not reduce Ba currents to values below Ca currents. It also appears that the introduction of Mg makes the measured currents and predicted surface concentrations saturate at higher bulk concentration values. Note that the theoretical curves were produced with the addition of only one more free parameter in the case of the pore model and no free parameters in the case without the pore.

Some features of the theoretical curves led us to favor the "fit" obtained with the pore present. Most prominent is the reduction in the tendency towards saturation of surface concentration for Ca at very low bulk concentrations. In addition, the theoretical curves for the case with no pore actually predict a juxtaposition of the Ca and Ba data at low bulk concentrations which is not observed experimentally. When the pore is introduced the fit between theory and experiment with respect to these details is improved.

The data and theoretical surface concentration curves predicted when Ba is held constant and Mg is varied are shown in Fig. 10*A*. The general shape of the theoretical and experimental curves are similar. In Fig. 10*B* we have included the $I-V$'s obtained in experiments where Ca and Ba were mixed in the presence or absence of Mg. Note that in both cases adding 10 mM Ca to 10 mM Ba actually decreased the current despite the fact that the number of permeant ions in the bulk solution has been doubled. Also note that both the shift and the reduction in current obtained when Ca is added to Ba is substantially greater when Mg is absent than when it is present. With the pore absent, the

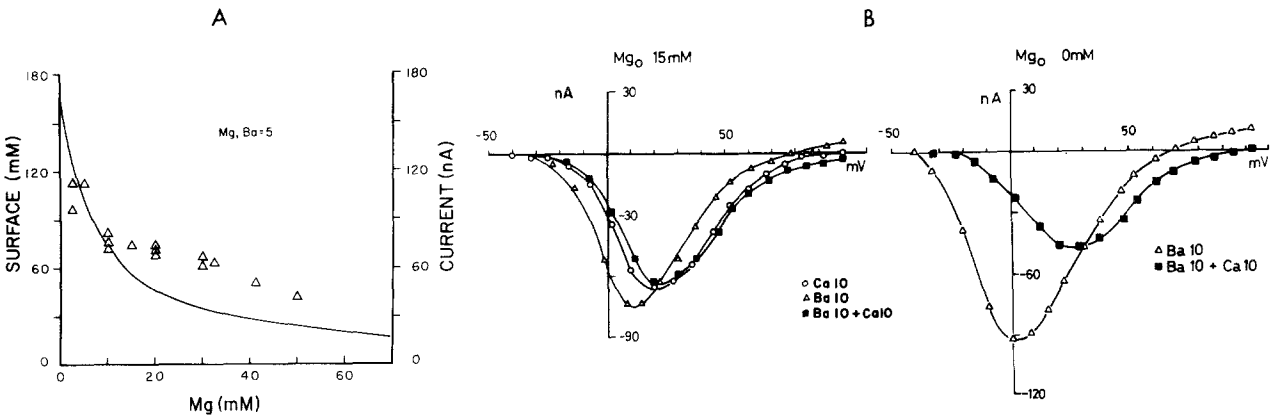

Fig. 10. (*A*): Effects of varying Mg on current-concentration relationship for I_{Ba}. The surface concentration prediction is for the pore model using the parameters listed in the legend to Figs. 8 and 9. (*B*): $I-V$ relationships in mixtures of Mg, Ca and Ba

model predicts a 30% reduction in the surface concentration of permeable ions when 10 mM Ca is added to 10 mM Ba in the absence of Mg. When $[Mg]_o$ is present the model predicts an almost constant surface concentration. The predictions for the percent reduction are thus somewhat smaller than those measured experimentally, but the predictions are close and they agree with the fact that adding Ca may actually reduce the measured current and that the presence of Mg may reduce this effect. Thus the theory tends to explain these somewhat surprising results.

Discussion

The shifts along the potential axis of the activation parameter A_∞, the descending limb of the $I-V$ curves and the peak of the $I-V$ curves were similar and these shifts are explained satisfactorily by the Gouy-Chapman equation with binding. The selectivity and saturation characteristics of the concentration-current relationships are explained when we consider the free surface concentration of the divalent cations. A modification of the theory was used to explain the Ca current-concentration curve at low concentrations which involved consideration of the effects of a charge-free channel mouth on the concentration at the mouth of the channel.

The shortcomings of GCt with binding as a theory are well-known (McLaughlin, 1977). McLaughlin (1977) indicates that in the case of the unmodified GCt without binding, it may be reasonable to overlook discrete charge effects since more macroscopic potentials are being examined, but in the case of binding it is possible that the local potentials around discrete charges may become important. In our case, where we have also studied permeation through the channel, it might be argued that the micro-environment of the channel is of interest and that a discrete charge model should be considered. The discrete charge model used by Brown (1974) may have been appropriate but he uses the linearized Poisson-Boltzman equation; i.e., he assumes that $\Psi << RT/F$. Sauve and Ohki (1979) constructed a discrete charge model and solved the problem numerically without linearization of the Poisson-Boltzman equation, and they discuss the relative merits of smeared versus discrete surface charge models. Fluctuations in discrete surface charge as proposed by Attwell and Eisner (1978) produced interesting changes in the potential dependence of the activation rate constants which would be consistent with results we have reported elsewhere (*see* Fig. 6, Brown et al., 1981). However, we are uncertain about the number of discrete sites per channel and we did not cover a sufficiently wide range of binding to test their proposal. Since the modified Gouy-Chapman smeared charge theory fitted our measurements very well despite its limitations and since our measurements were not sufficiently accurate to distinguish between a smeared charge and a discrete charge representation, the smeared charge model was used.

We did, however, apply the disc model modification of Apell et al. (1979) because of its simplicity. A limitation of the disc model is the assumption that $\Psi \ll RT/F$; nevertheless we felt that this solution was sufficiently realistic to examine the effects of a charge-free region on the concentration at the mouth of a channel. By adding one more free parameter, the disc radius, we are able to provide a better fit of the current vs. concentration data.

Apell et al. (1979) rejected the idea that a reduction in the surface potential in the center of the channel could account for the decrease in Cs

current that they observed at low concentrations. In their case, however, they were using only singly charged ionic species; thus, the Debye length was much larger than in our case and it was very close to the estimated gramicidin channel radius of 10 Å. In our case, with a shortened Debye length, we calculated an effect using a reasonable value for the channel radius. We should point out that Apell et al. (1979) offer several other plausible explanations for the reduction in current at low external concentrations.

Despite the shortcomings of the theory at the microscopic level its widespread usage allows some comparisons among gating of different channels to be made. Thus, our results for Ψ, σ and K for Ca are similar to those obtained by Ohmori and Yoshii (1977) for Na and Ca channels and by Hille et al. (1975) for the Na channel, although the results indicate a greater surface charge density than is found near K channels (Gilbert & Ehrenstein, 1969). We should note that other models of surface binding sites have appeared in the literature. McLaughlin et al. (1981) assume that divalent cations bind to monovalent anionic sites on the membrane. This model allows them to describe the sign change in the net surface charge that has been observed experimentally using artificial membranes. Our measurements will not allow us to discriminate between their model and the one used by Gilbert and Ehrenstein (1969); in the case of the model of McLaughlin et al. (1981), we may fit our data equally well with a binding constant for Ca that is simply reduced by a factor of $^1/_2$.

In our application of GCt we did not consider the possibility that Na or other monovalent cations bind to the membrane adjacent to the Ca channel as well as exerting a screening effect. For example, the surface potential of a pure phosphatidylserine or phosphatidylglycerol bilayer is not more negative than -100 mV but is in fact only about -85 mV in 0.1 mM NaCl (Eisenberg, Gresalfi, Riccio & McLaughlin, 1979) due presumably to the binding of Na. Binding of monovalent cations will alter quantitative conclusions about the magnitude of the surface potential and the magnitude of the binding constants for the divalent cations, but the general conclusions presented here remain valid.

We should point out that the assumption of zero binding by Ba, Sr and Mg is quite arbitrary. By measuring the change in gating parameters we measure only relative changes in the surface potential values and not absolute values. Recent evidence from other types of physical measurements on artificial membranes indicates that there may be much more binding than previously thought (McLaughlin et al., 1981). McLaughlin et al. (1981) argue that a reasonable binding constant for Ca to phosphatidylserine (PS), a major constituent in biological membranes, is approximately 10 M^{-1}. We did additional calculations assuming this value and we obtained reasonable fits to our data with a different set of parameter values. We used a σ of $1\,e^-/90$ Å^2, a maximum Ψ of -113 mV, a β of $+56$ mV, a binding constant for Ca of 10 M^{-1}, and binding constants for Ba, Mg and Sr of 2 M^{-1}. Which set of values is most appropriate for biological tissue is not known. Using our methods, testing the validity of binding by Ba, Sr and Mg would require finding a divalent cation which showed less voltage shifting than these species and thus indicated less binding.

Ohmori and Yoshii (1977) calculated relative permeabilities for Ca, Sr and Ba using a modified form of the constant field equation which takes into account surface potential effects as suggested by Frankenhaeuser (1960). After correction, they found the relative permeabilities to be 1.0, 0.56 and 0.21 for Ca, Ba and Sr, respectively. Okamoto et al. (1977) measured divalent cation currents in mammalian, tunicate and sea urchin oocytes and argued that after correction for surface potential effects and other effects there were no significant differences between species and that the permeability sequence was Ca > Sr > Ba. In our case, the ratio of the currents obtained are very close to the ratios of the surface concentrations predicted (Fig. 9); thus, we would calculate the same permeability constant for each species. The deviations of the shape of the current-concentration data from the surface concentration-bulk concentration predictions probably arrive as a result of the simplifications used in the mathematical formulation rather than as a result of the physical properties of the membrane. Thus, the permeability sequence of the Ca channel is most probably due to binding at the membrane surface in a manner consistent with the surface-charge theory rather than binding at a channel site as previously supposed (Hagiwara, 1975; Akaike et al., 1978; Kostyuk, 1980). Also, the saturation of the current-concentration relationship may arise due to the saturation of the surface concentration rather than the saturation of a channel binding site. This is not to say that the Ca channel has no cation specific binding sites for divalent cations. The fact that Co reduces the relative permeability to Ba ion may be explained by such a site.

The effects of Mg on I_{Ba} and I_{Ca} provide an interesting test of the theory. We allow no binding of Mg at the membrane surface; thus, it acts through a screening effect only. The shifts pro-

duced when Mg is present in the solution are very close to the predicted values, indicating that the simple Gouy-Chapman theory quantifies the surface potential accurately. The currents obtained agree in several aspects. In Fig. 9, we see that Mg reduces I_{Ca} much less than it reduces I_{Ba}, and the shapes of the current-concentration curves are affected by Mg in such a way as to increase the concentration at which saturation occurs (Figs. 9*A* and *B*). In Fig. 10*A*, the reductions in current produced by increasing the external Mg agree with the reduction in surface concentration predicted. Finally, in Figs. 5 and 10*B*, we see that the presence of Mg very much reduces the effect on the voltage shift and the change in peak current when either 10 mM Ba or 10 mM Ca are added to a solution containing 10 mM Ba. Hence, surface charge theory agrees quantitatively with every aspect of the effects of adding Mg, and we can conclude that the so-called "blocking" action of Mg does not occur as a result of competitive binding at a channel site; it occurs primarily as a result of the screening of external surface charge.

Another feature of the results obtained with Mg is worth noting. At high Mg values, $[Mg]_o = 35$ mM, we found that the shifting produced by varying the amount of Ba was much less than in the case of zero Mg, but it was still present. Although it hasn't been plotted the theoretical predictions for varying Ca in the presence of high Mg shows an even larger effect. Thus, in preparations immersed in artificial seawater with $[Mg]_o = 50$ to 1000 mM the surface potential effects are expected to be reduced but not eliminated. The results show that it is virtually impossible to screen surface charge so as to examine permeation of the Ca channel in the absence of any surface potential.

Begenisich (1975) has investigated surface charge effects on both the activation curves and permeation for both Na and K currents. He found that the instantaneous $I-V$ relationships for K were not rectified nearly as much as one would predict using surface concentration values in the constant field equation. Likewise the Na instantaneous $I-V$ was not altered as expected. These results indicate a larger effect of surface charge on activation than permeation, and he concluded that the "voltage sensing" elements for these currents were electrically far removed from the pores, a conclusion also reached by Hille (1975). Our results are consistent with this conclusion. The shift in the activation parameters indicates a greater surface charge effect than that indicated by the current-bulk concentration relationship. We required a charge-free disk to describe our current-bulk concentration relationships.

Our analyses have assumed relatively simple permeation characteristics for the Ca channel. We have assumed that the Ca channel obeys Independence and the inward current is simply proportional to the surface concentration of permeable ions. Considering the complexities that have been discovered in the Na and K channels that are unexplained by simple electro-diffusion theories (*see* the collection of papers edited by Stevens & Tsien, 1979, for a representative review), it is unlikely that the Ca channel will show no such complexities even after accounting for surface charge effects. For example, if there are indeed interactions between Na^+ ions that limit the number of Na ions at sites in the channel as proposed by Hille (1975), then in the case of a divalent ion one would expect an even greater repulsion. One significant deviation may be the effect of Co that we describe. Nevertheless, at the very least we conclude that permeation mechanisms can be examined only upon consideration of surface charge effects, and we re-emphasize that the latter cannot be eliminated experimentally.

The shifts of the inactivation parameter $h_\infty(v)$ between I_{Ba} and I_{Ca} were similar to the shifts in the activation parameter and suggest that the external charged sites exert equivalent effects on the membrane sturctures responsible for these two processes. Perfusion with intracellular EGTA did not shift $h_\infty(v)$ for I_{Ca} to more positive potentials although prepulse durations had to be increased to achieve a given level of steady inactivation. The necessity for increasing prepulse duration was expected since $EGTA_i$ prevents Ca current-dependent inactivation (Brown et al., 1981). The absence of a shift in the steady-state inactivation-potential curves leads us to conclude that the internal site with which Ca reacts does not exert an effect on the Ca channel via a surface charge mechanism. In this respect it is of interest that intracellular perfusion with a wide variety of divalent cations produced no shifts in V_p consistent with the presence of an internal surface charge (Akaike & Yatani, *manuscript in preparation*) although currents were reduced. These observations are consistent with the findings of Begenisich and Lynch (1974) for Na and K channel of squid axon although they differ from the conclusion of Chandler, Hodgkin and Meves (1965). The effects of internal Ca on inactivation (Brown et al., 1981) would appear to involve a specific chemical reaction that does not have observable surface potential effects.

To summarize, surface charge contributes importantly to gating, selectivity and saturation in the Ca channel. Previous "binding site" models of the Ca channel have been used to describe

current-concentration relationships alone whereas the surface charge model, by comparision, involves two independent measurements – voltage shifting and current magnitude. Thus, surface charge theory is more rigorously tested than binding site theory and agrees in most aspects with the measurements. We conclude that future investigations into the properties of the Ca channel should begin with the assumption of surface charge effects.

We wish to acknowledge the help of Dee Kelly, Janet McLellan and Harold Henderson in the preparation of this paper. This work was supported by NIH grants NS-11453 and HL-25145.

References

Akaike, N., Lee, K., Brown, A.M. 1978. The calcium current of *Helix* neuron. *J. Gen. Physiol.* **71**:509–531

Apell, H.J., Bamberg, E., Lauger, P. 1979. Effects of surface charge on the conductance of the gramicidin channel. *Biochim. Biophys. Acta* **552**:368–378

Attwell, D., Eisner, D. 1978. Discrete membrane surface charge distributions. Effect of fluctuations near individual channels. *Biophys. J.* **24**:869–875

Begenisich, T. 1975. Magnitude and locations of surface charges on myxicola giant axons. *J. Gen. Physiol.* **66**:47–65

Begenisich, T., Lynch, C. 1974. Effects of internal divalent cations on voltage-clamped squid axon. *J. Physiol. (London)* **62**:675–689

Brehm, P., Tillotson, D., Eckert, R. 1978. Calcium mediated inactivation of calcium current in paramecium. *J. Physiol. (London)* **306**:193–204

Brown, A.M., Morimoto, K., Tsuda, Y., Wilson, D.L. 1981. Calcium current dependent and voltage-dependent inactivation of Ca channels. *J. Physiol (London)* **320**:193–218

Brown, A.M., Tsuda, Y., Morimoto, K., Wilson, D.L. 1982. Actions of calcium ion on gating and permeation of the calcium channel. *In:* The Mechanism of Gated Calcium Transport across Biological Membranes. pp. 53–62. Academic Press, New York

Brown, R.H., Jr. 1974. Membrane surface charge: Discrete and uniform modelling. *Prog. Biophys. Mol. Biol.* **28**:343–370

Byerly, L., Hagiwara, S. 1982. Calcium currents in internally perfused nerve cell bodies of Limnea Stagnalis. *J. Physiol. (London)* **322**:503–528

Chandler, W.K., Hodgkin, A.L., Meves, H. 1965. The effect of changing the internal solution on sodium inactivation and related phenomena in giant axons. *J. Physiol. (London)* **180**:821–836

Eckert, R., Tillotson, D. 1978. Potassium activation associated with intraneuronal free calcium. *Science* **200**:437–439

Eisenberg, M., Gresalfi, T., Riccio, T., McLaughlin, S. 1979. Adsorption of monovalent cations to bilayer membranes containing negative phospholipids. *Biochemistry* **18**:5213–5223

Frankenhaueser, B. 1960. Sodium permeability in toad nerve and in squid nerve. *J. Physiol. (London)* **152**:159–166

Frankenhaueser, B., Hodgkin, A.L. 1957. The action of calcium on the electrical properties of squid axons. *J. Physiol (London)* **137**:218–244

Gilbert, D.L., Ehrenstein, G. 1969. Effect of divalent cations on potassium conductance of squid axons: Determination of surface charge. *Biophys. J.* **9**:447–463

Grahame, D.C. 1947. The electrical double layer and the theory of electrocapillarity. *Chem. Rev.* **41**:441–501

Hagiwara, S. 1975. Ca-dependent action potential. *In:* Membranes – A Series of Advances, third Edition. G. Eisenberg, editor. pp. 359–382. Marcel Dekker, New York

Hagiwara, S., Byerly, L. 1981. Calcium channel. *Annu. Rev. Neurosci.* **4**:69–125

Hille, B. 1975. Ionic selectivity, saturation and block in sodium channels – A four barrier model. *J. Gen Physiol.* **66**:535–560

Hille, B., Woodhull, A.M., Shapiro, B. 1975. Negative surface charge near sodium channels of nerve divalent ions, monovalent ions, and pH. *Philos. Trans. R. Soc. London B* **270**:301–318

Hodgkin, A.L., Huxley, A.F. 1952. A quantitative description of membrane current and its application to conduction and excitation in nerve. *J. Physiol. (London)* **117**:500–544

Kostyuk, P.G. 1980. Calcium ionic channels in electrically excitable membranes. *Neuroscience* **5**:945–959

Kostyuk, P.G., Doroshenko, P.A., Ponomazev, V.N. 1980. Surface charge in the region of localization of calcium channels of the somatic membrane of mollusc neurons. *Doklady Acad. Sci. USSR* **250**:464–467

Kostyuk, P.G., Krishtal, O.A., Doroshenko, P.A. 1974. Calcium currents in snail neurones. *Pfluegers Arch.* **348**:95–104

Kostyuk, P.G., Krishtal, O.A., Pidoplichko, V.I. 1981. Calcium inward current and related charge movements in the membrane of snail neurons. *J. Physiol. (London)* **310**:403–421

Lee, K.S., Akaike, N., Brown, A.M. 1980. The suction pipette method for internal perfusion and voltage clamp of small excitable cells. *J. Neurosci. Meth.* **2**:51–78

McLaughlin, S. 1977. Electrostatic potentials at membrane solutions interfaces. *Curr. Top. Membr. Transp.* **9**:71–144

McLaughlin, S., Mulrine, N., Gresalfi, T., Vaio, G., McLaughlin, A. 1981. Adsorption of divalent cations to bilayer membranes containing phosphatidylserine. *J. Gen. Physiol.* **77**:445–473

McLaughlin, S., Szabo, G., Eisenman, G. 1971. Divalent ions and the surface potential of charged phospholipid membranes. *J. Gen. Physiol.* **58**:667–687

Mozhaeyeva, G.N., Naumov, A.P. 1970. Effect of surface charge on the steady state potassium conductance of nodal membrane. *Nautre (London)* **228**:164–165

Ohmori, H., Yoshii, M. 1977. Surface potential reflected in both gating and permeation mechanisms of sodium and calcium channels of the tunicate egg cells membrane. *J. Physiol. (London)* **267**:429–463

Okamoto, H., Takahashi, K., Yamashita, N. 1977. Ionic currents through the membrane of the mammalian oocyte and their comparison with those in the tunicate and sea urchin. *J. Physiol. (London)* **267**:467–495

Sauve, R., Ohki, S. 1979. Interactions of divalent cations with negatively charged membrane surfaces. I. Discrete charge potential. *J. Theor. Biol.* **81**:157–179

Stern, Z. 1924. *Electrochemistry* **30**:508

Stevens, C.F., Tsien, R.W. 1979. Membrane Transport Processes. Vol. 3: Ion Permeation Through Membrane Channels. Raven Press, New York

Tillotson, D. 1979. Inactivation of Ca conductance dependent on entry of Ca ions in molluscan neurons. *Proc. Natl. Acad. Sci. USA* **3**:1497–1500

Tsuda, Y., Wilson, D., Brown, A.M. 1982. Calcium channel tail currents in snail neurons. *Biophys. J.* (*Abstr.*) **37**:181A

Wilson, D., Tsuda, Y., Brown, A.M. 1982. Activation of Ca channels in snail neurons. *Biophys. J.* (*Abstr.*) **37**:181A

Received 8 June 1982; revised 8 September 1982